Available online at www.sciencedirect.com
SCIENCE DIRECT®
Journal of Non-Crystalline Solids 326&327 (2003) 159–164
JOURNAL OF NON-CRYSTALLINE SOLIDS
www.elsevier.com/locate/jnoncrysol

Electrical conductivity of $Ag_x(As_{40}Se_{60})_{100-x}$ bulk glasses

V. Zima [a,*], T. Wágner [b], Mil. Vlček [a], L. Beneš [a], S.O. Kasap [c], M. Frumar [b]

[a] *Joint laboratory of Solid State Chemistry of Czech, Academy of Sciences and University of Pardubice, Studentská 84, 53210 Pardubice, Czech Republic*
[b] *University of Pardubice, Legion's sq. 565, 53210 Pardubice, Czech Republic*
[c] *University of Saskatchewan, Saskatoon, Canada S7N 5A9*

Abstract

The samples of $Ag_x(As_{40}Se_{60})_{100-x}$ ($x = 1$–30) bulk glasses were prepared by a standard melt-quenching technique. Thermal and electrical properties were studied on the prepared glasses. Temperature-modulated differential scanning calorimetry was used to measure glass transition, cold crystallization and melting temperatures of the prepared samples. Electrical transport properties were studied by an impedance spectroscopy and dc conductivity measurements. Activation energies of the conductivity were calculated from Arrhenius plots. One-semicircle impedance spectra were found for all the glasses studied except that with 9 at.% of silver. For this sample impedance spectra with two semicircles were obtained. This phenomenon is discussed in the terms of Bauerle's easy path theory. The compositional dependence of the conductivity showed an increase of the conductivity with increasing silver content.

PACS: 71.55.Jv; 72.15.Cz; 72.60.+g

1. Introduction

Recent development of solid state batteries, memory devices, electrochemical devices, catalysts, and anticorrosion media leads to necessity to investigate electronic properties of systems with solid–solid interfaces of materials having often character of solid ionic conductors [1–4]. One of the most promising classes of materials for those purposes seems to be chalcogenide glasses containing silver [5–8]. In many cases, one of the important electronic properties, conductivity, cannot be determined by conventional dc methods because of the polarization effects on the interface between the sample and the electrodes. To avoid these problems, it is convenient to use impedance spectroscopy and to measure ac conductivity. To characterize sample behavior it is always necessary to have information about some materials properties (e.g., thermal and structural) of the samples obtained with other analytical methods such as temperature-modulated DSC or X-ray diffraction.

Some compositions (e.g., Ag_3AsSe_3) of the Ag–As–Se systems have been studied previously using impedance spectroscopy [9–11]. As far as we know there is no such study on the glasses with general

* Corresponding author. Tel.: +42-40 603 6146; fax: +42-40 603 6011.
E-mail address: vitezslav.zima@upce.cz (V. Zima).

0022-3093/$ - see front matter © 2003 Elsevier B.V. All rights reserved.
doi:10.1016/S0022-3093(03)00398-3

formula $Ag_x(As_{40}Se_{60})_{100-x}$ of compositional span $x = 1$–30.

2. Experimental techniques

The samples of the system $Ag_x(As_{40}Se_{60})_{100-x}$, where $x = 0$–30 at.% were prepared from 5N elements by a standard melt-quenching technique with the starting materials placed in evacuated quartz ampoules [12]. Thermal properties of the samples were measured using a modulated differential scanning calorimetry (MDSC) of the samples placed in aluminum crimped pans. The heat flow from the samples was measured in modulated and non-modulated regimes. An X-ray diffractometer D8 Advance (Bruker AXS) with a goniometer radius of 217.5 mm, secondary graphite monochromator, and Cu Kα radiation was used for powder diffraction measurements. The samples were measured in bulk and powder forms placed on the surface of a Si monocrystal. The diffractometer was equipped with an attachment that allowed X-ray diffraction measurements at different temperatures.

The samples for dc and ac measurements were in the form of parallelepipeds with dimension of 3–5 mm. The sides of the samples in contact with metal electrodes were coated with a graphite paste.

The dc conductivity measurements were performed on a solid state electrometer Keithley 610 C, which measures current in the range from 0.3 to 1×10^{-14} A.

An impedance meter Tesla BM 653 working in the frequency region from 20 to 5×10^5 Hz with an input signal level of 0.5 V connected on-line with a computer through an A/D interface was used for the conductivity measurements. The impedance meter provides values of modulus $|Z|$ and phase angle φ. From these values, the real (Z_{Re}) and imaginary (Z_{Im}) parts of the impedance were calculated. The experimental impedance data can be analyzed as impedance of an equivalent circuit made up of ideal resistors, capacitors, or various distributed circuit elements. Resistance of such a circuit can be associated for instance with a bulk conductivity of the material and a capacitance with a space charge polarization. In a complex impedance plot (i.e., a plot of imaginary vs. real parts of the impedance), an ideal circuit, consisting of a resistance R connected in parallel with a capacitance C, is represented by a semicircle lying on the x-axis. The total impedance Z of this circuit then depends on an angular frequency ω of the input signal by the equation

$$Z = \frac{R}{1 + j\omega RC}. \tag{1}$$

In real systems, which have its physical properties often distributed, the complex impedance plot shows an arc with a center depressed under the x-axis. In the corresponding equivalent circuit, the capacitance is then replaced by a so-called constant phase element CPE for which the impedance Z_{CPE} can be expressed as

$$Z_{CPE} = \frac{R}{(j\omega\tau_R)^{\psi}}, \tag{2}$$

where τ_R is a mean relaxation time (when Z_{Im} reaches its maximum value, then $\tau_R = \omega^{-1}$) and $\psi = 1 - \alpha$, where α is a measure of distribution of relaxation times τ. The equation (1) can be rewritten for a circuit composed of parallel R and CPE elements as

$$Z = \frac{R}{1 + (j\omega\tau_R)^{\psi}}. \tag{3}$$

For more complex systems, a combination of various circuit elements, i.e. C, R, and CPE with corresponding equations can be used. The parameters (R, τ_R, ψ) are estimated from the experimental Z vs. ω dependence using a complex non-linear squares method [13].

The ac conductivity (thereafter denoted as σ) of the samples was measured on the $Ag_x(As_{40}Se_{60})_{100-x}$, bulk samples, in the frequency region from 0.5 MHz to 10 Hz at temperatures from 0 to 100 °C.

3. Results and discussion

The sample of $As_{40}Se_{60}$ glass with 1 at.% of Ag is too resistive, and therefore the conductivity measurements could not be carried out on this sample. In all other cases, the imaginary vs.

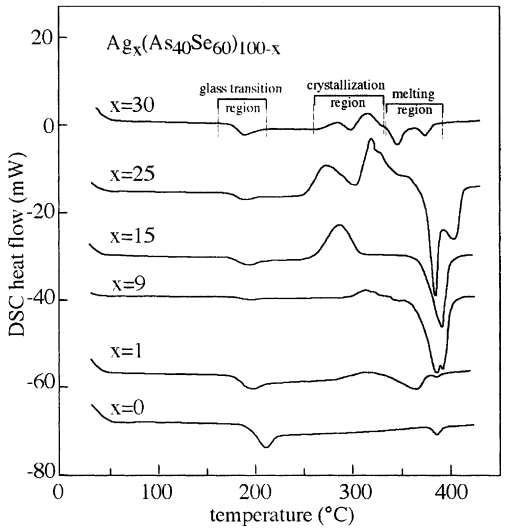

Fig. 1. DSC curves of the studied samples in the $Ag_x(As_{40}Se_{60})_{100-x}$ system.

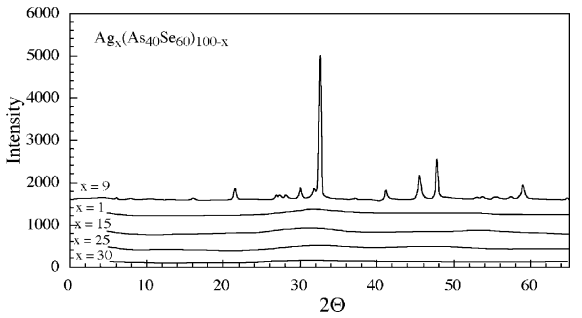

Fig. 2. X-ray diffraction curves of the studied samples in the $Ag_x(As_{40}Se_{60})_{100-x}$ system.

real parts of the impedance shows arc-shaped curves.

From DSC measurements (Fig. 1) and X-ray powder diffraction (Fig. 2) data it is obvious that all the samples are glassy except the sample with 9 at.% of silver. Two recrystallization peaks observed by DSC mean that the recrystallization of the low-temperature modification occurs with a transition to a high-temperature modification, which is followed by melting [14].

As follows from the DSC technique (Fig. 1) and X-ray powder diffraction (Fig. 2), $As_{40}Se_{60}$ with 9 at.% Ag contains both crystalline and glassy phases. The glass was prepared in the same manner as in the previous paper [12]. Nevertheless, due to higher amount of the reaction mixture, the glass partially crystallized. The composition of this glass is on the edge of a glass-forming region [15] as can be deduced from the ternary phase diagram and the crystalline phase is richer with silver.

Two arcs were observed in the complex impedance plot of the experimental data for the $As_{40}Se_{60}$ glass doped with 9 at.% Ag (Fig. 3), in contrast to the $As_{40}Se_{60}$ glasses with different content of silver, where only one arc was observed. The smaller semicircle, in the high-frequency region, corresponds to a phase with higher conductivity. The larger semicircle in the low-frequency region represents a phase with lower conductivity. As found from the thermal behavior of the ac conductivity, both phases obey Arrhenius law in the temperature range studied (see Fig. 4). The values of the activation energy of the conductivity ΔE were calculated using an equation

$$\sigma = \sigma_0 T^{-1} \exp(-\Delta E/kT) \quad (4)$$

and are roughly equal for both phases (Table 1). This phenomenon can be explained by a Bauerle's easy path theory [16]. According to this theory, a sample is composed of grains with grain boundary

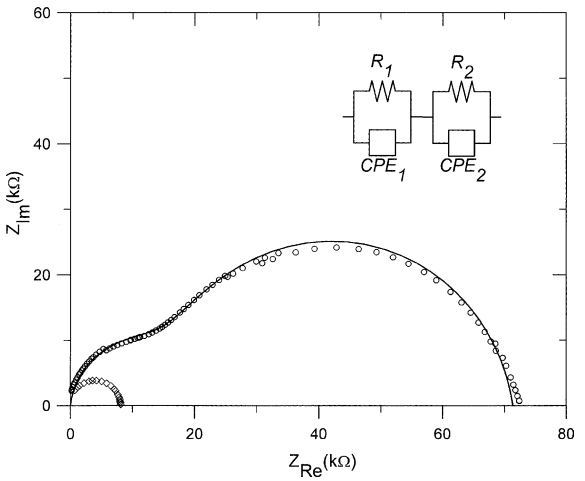

Fig. 3. Double-arc impedance spectrum (circles) of the studied sample of $Ag_9(As_{40}Se_{60})_{91}$ at 40 °C. In the inset, an equivalent circuit is depicted comprising resistance (R) and constant-phase (CPE) elements. For comparison, the impedance data for the $Ag_{25}(As_{40}Se_{60})_{75}$ sample at 40 °C is shown (diamonds).

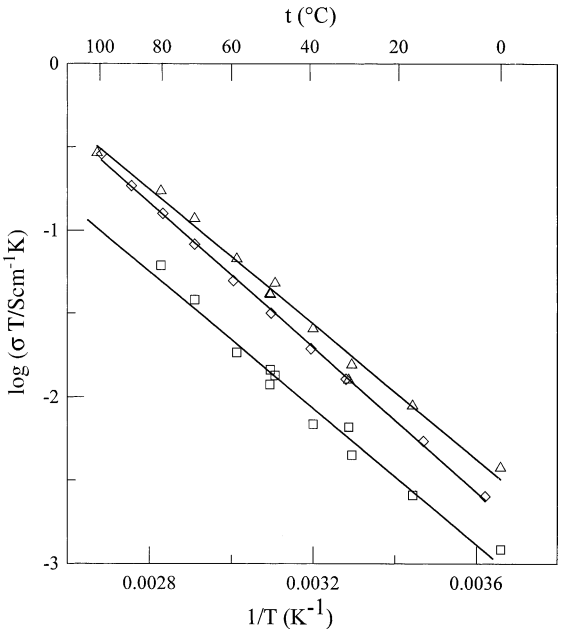

Fig. 4. Arrhenius plot for $Ag_9(As_{40}Se_{60})_{91}$. Triangles and squares represent the conductivity of the high-frequency and low-frequency regions, respectively, of the impedance spectrum of the pristine sample. Diamonds correspond to the conductivity of the sample heated to 120 °C.

regions, which are filled with a phase different from the phase forming the grains; these regions are called easy paths. In the impedance spectrum, the high-frequency semicircle corresponds to the phase forming the grains and the low-frequency part expresses electrical properties of the grain boundaries. In this case, one can presume that the sample is composed of crystalline grains and the area between them is filled with a glassy phase. Thus, the resistance calculated from the high-frequency semicircle expresses the resistance of an interior of the grains (i.e., the crystalline phase, richer with Ag), while the low-frequency semicircle reflects the resistance of the grain boundary (the glassy phase, with lower Ag content). As follows from the ac conductivity measurements, the glassy phase has lower conductivity.

By heating the sample up to 120 °C, the impedance spectrum changes and only one arc is observed in the complex impedance plot. The conductivity calculated from this semicircle lies between the values found for the crystalline and glassy phases of the original sample (Fig. 4). Most probably, a phase transition occurs during heating and the sample becomes fully crystalline or the effect could also be related to growth of some structural clusters in the annealed glass. The net content of Ag in this thermally treated sample is of course somewhat lower than in the crystalline phase forming grains in the pristine sample and, consequently, the conductivity of the thermally treated sample is lower than the conductivity of the crystalline phase in the pristine sample.

The impedance spectrum of $As_{40}Se_{60}$ glass with 15 at.% of Ag reveals only one semicircle in the measured frequency range. The resistance of this

Table 1
Conductivity parameters calculated for the $Ag_x(As_{40}Se_{60})_{100-x}$ glasses

x (at.% Ag)	A	B	E_a [eV]	σ_{rt} [S cm^{-1}]
9[a]	4.93	−2028	0.402	4.504×10^{-5}
9[b]	4.50	−2051	0.407	1.401×10^{-5}
9[c]	5.25	−2173	0.431	3.071×10^{-5}
15	4.46	−2352	0.467	1.250×10^{-6}
25[d]	0.18	−556.8	0.110	6.887×10^{-5}
25[e]	3.77	−1742	0.346	
30[d]	0.12	−459.4	0.092	1.273×10^{-4}
30[e]	1.49	−878.5	0.174	

x – amount of silver in $Ag_x(As_{40}Se_{60})_{100-x}$, A, B – parameters of the linear regression for the equation $\log(\sigma T) = A + BT^{-1}$, E_a – activation energy of conductivity, σ_{rt} – conductivity at room temperature.

[a] High-frequency arc.

[b] Low-frequency arc.

[c] After heating to 120 °C.

[d] Low-temperature part.

[e] High-temperature part.

glassy sample is higher than that for As_2S_3 with 9 at.% Ag and also the activation energy (calculated from the Arrhenius dependence, which is linear in the temperature range studied) is higher. This indicates that the glassy samples are generally less conductive than the crystalline samples even with lower amount of Ag.

With further increasing content of silver, the conductivity of the samples increases. For $As_{40}Se_{60}$ glass with 25 at.% of silver, it is about one order higher than that for $As_{40}Se_{60}$ with 15 at.% of Ag. The Arrhenius plot for $As_{40}Se_{60}$ with 25 at.% of silver shows two distinct areas of linear dependencies below and above 60 °C (Fig. 5) indicating two different conductivity mechanisms. The detailed study of this behavior is under way.

The role of Ag^+ ions as charge carriers was confirmed by the dc measurements. A current was measured on the $Ag_{25}(As_{40}Se_{60})_{75}$ sample, where one electrode is formed by a silver film deposited on one side of the sample. Two experiments were performed, both with constant voltage applied (Fig. 6).

Experiment 1: The Ag^+ ions from the sample are discharged into the silver film forming a cathode. The change of current values with time of loading under constant voltage is typical of behavior of ionic conductors with blocking electrodes. The current decreases exponentially and reaches steady state after about 1 day.

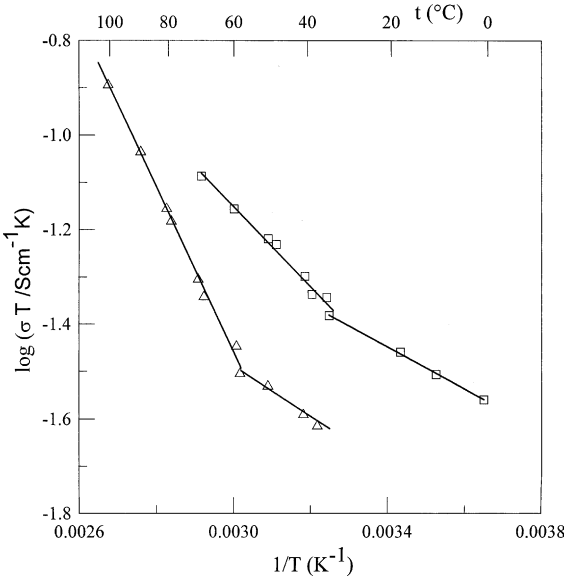

Fig. 5. Arrhenius plot for the $Ag_x(As_{40}Se_{60})_{100-x}$ system with 25 (triangles) and 30 (squares) at.% of silver.

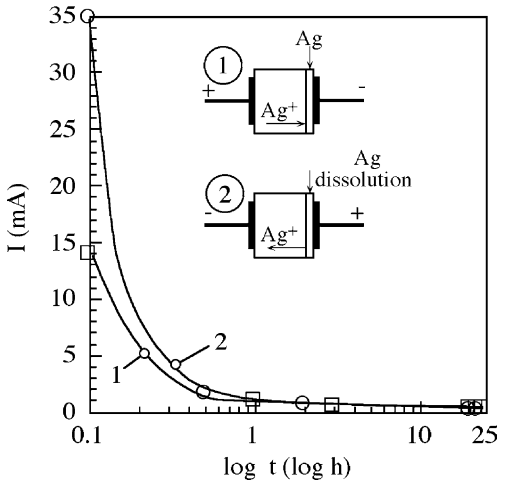

Fig. 6. Typical dc-current vs. time curves of $Ag_9(As_{40}Se_{60})_{91}$.

Experiment 2: The electric field applied to the sample has opposite polarity than in Experiment 1. The Ag^+ ions are formed at a silver-film anode in addition to the Ag^+ ions present in the sample. The concentration of the charge carriers is therefore higher than in Experiment 1 and, consequently, the starting current is higher than that in Experiment 1. After more than one day, the current reaches steady state with the same value as in Experiment 1.

In steady state, the Ag^+ ions are localized at the interface of the cathode, which is a blocking electrode for them and the net steady-state conductivity is only electronic. The dc conductivity in steady state at room temperature (i.e., only electronic conductivity) is much lower than that measured by ac technique (which represents a sum of electronic and ionic conductivities).

The sample of $As_{40}Se_{60}$ glass with 30 at.% of Ag has the highest content of silver among the samples studied and also the highest conductivity and the lowest activation energy in the high-temperature region (Table 1). The Arrhenius plot is similar to that for $As_{40}Se_{60}$ with 25 at.% Ag (Fig. 5). The

reversible change of the conductivity mechanism is observed at around 35 °C.

4. Conclusion

The chalcogenide glasses in the compositional span of $x = 1$–30 for $Ag_x(As_{40}Se_{60})_{100-x}$ were prepared and characterized. The DSC and X-ray diffraction techniques have shown that the samples are in a glassy state. Only the sample with 9 at.% of Ag is a heterogeneous mixture of the crystalline and glassy phases. Impedance spectroscopy proves itself as a very sensitive tool for this kind of inhomogeneity. A double-arc impedance spectrum has changed to a one-arc impedance spectrum after heating to 120 °C. The samples have increasing conductivity with increasing silver content and temperature. DC measurements confirmed the role of Ag^+ ions as charge carriers.

Acknowledgements

The authors thank grant V.Z. no. 253100001, grants 203/02/0087, 203/00/0085 of the Grant Agency of Czech Republic and to Research Centre project LN00A028.

References

[1] M.D. Ingram, in: M. Cable, J.M. Parker (Eds.), High-Performance Glasses, Chapman and Hall, New York, 1992, p. 133.
[2] A. Pradel, M. Ribes, Mater. Sci. Eng. B3 (1989) 45.
[3] A. Levasseur, M. Menetrier, R. Dormoy, G. Meunier, Mater. Sci. Eng. B3 (1989) 5.
[4] M. Balkanski, Mater. Sci. Eng. B3 (1989) 1.
[5] M. Mitkova, M.N. Kozicki, J. Non-Cryst. Solids 299–302 (2002) 1023.
[6] T. Usuki, O. Uemura, S. Konno, Y. Kameda, M. Sakurai, J. Non-Cryst. Solids 293–295 (2002) 799.
[7] M. Kawasaki, J. Kawamura, Y. Nakamura, M. Aniya, Solid State Ionics 123 (1999) 259.
[8] A. Giridhar, S. Mahadevan, J. Non-Cryst. Solids 197 (1999) 228.
[9] A. Yoshiasa, Mineralog. J. 40 (1989) 293.
[10] Y.G. Vlasov, E.A. Bychkov, Solid State Ionics 14 (1984) 329.
[11] V. Zima, Sci. Papers of the University of Pardubice, 2A, 1996, p. 297.
[12] T. Wágner, M. Frumar, S.O. Kasap, J. Non-Cryst. Solids 256&257 (1999) 160.
[13] J.R. MacDonald, W.B. Johnson, in: J.R. MacDonaLD (Ed.), Impedance Spectroscopy, Wiley, New York, 1987, p. 17.
[14] R. Keim, Gmelin Handbook, Silver—part 4B, Springer, Berlin, 1974, p. 67.
[15] Z.U. Borisova, Glassy Semiconductors, Plenum, New York, 1981.
[16] J.E. Bauerle, J. Phys. Chem. Solids 30 (1969) 2657.